FLEXURAL TESTING OF HIGH STRENGTH REINFORCED CONCRETE BEAMS STRENGTHENED WITH CFRP SHEETS

*S.H. Hashemi**

Faculty of Engineering, Arak University
P.O. Box 38139, Arak, Iran
hamidhashemi55@yahoo.com

R. Rahgozar and A.A. Maghsoudi

Department of Civil Engineering, University of Kerman
P.O. Box 76169-14111, Kerman, Iran
rahgozar@mail.uk.ac.ir - maghsoudi.a.a@mail.uk.ac.ir

*Corresponding Author

Abstract The objective of this study is to investigate the effectiveness of externally bonded CFRP sheets to increase the flexural strength of reinforced high strength concrete (HSC) beams. Four-point bending flexural tests to complete failure on six concrete beams, strengthened with different layouts of CFRP sheets were conducted. Three-dimensional nonlinear finite element (FE) models were adopted by ANSYS to examine the behavior of the test beams. More specifically, the strength and ductility of the beams is investigated, as the number of FRP layers and tensile reinforcement bar ratio changed. With the exception of the control beam, one to four layers of CFRP were applied to the specimens. The ductility characteristics of the test beams were evaluated in terms of the displacement, curvature and energy ductility index. It was found that for all the reported beams, the energy ductility value is about two times higher than the displacement ductility values. The crack patterns in the beams are also presented. The load deflection plots obtained from numerical study show good agreement with the experimental results.

Keywords Ductility, Finite Element Model, FRP, High Strength Concrete

چکیده   هدف این تحقیق بررسی اثر ورق های CFRP در مقاوم‌سازی خمشی تیرهای بتن مسلح حاوی بتن با مقاومت بالا می‌باشد. شش تیر بتنی دارای سطح مقطع، طول و میزان میله گرد فشاری و برشی یکسان حاوی بتن با مقاومت بالا، پس از مقاوم‌سازی تحت آزمایش خمش چهار نقطه ای تا لحظه شکست قرار گرفته و مورد بررسی قرار گرفته‌اند. از شش نمونه ذکر شده که به دو سری از نظر میزان میله گرد کششی تقسیم شده‌اند یک نمونه از هر سری بدون FRP به عنوان نمونه شاهد و دو نمونه دیگر با یک و چهار لایه FRP مقاوم‌سازی شده‌اند. شاخص شکل پذیری نمونه‌ها توسط نتایج خیز، انحناء و انرژی محاسبه و ارائه شده است. نتایج آزمایش‌ها نشان دهنده عملکرد مناسب ورق‌های FRP در افزایش مقاومت نهایی، کاهش شدید عرض ترک، کاهش خیز و بطور کلی بهبود شرایط در حالت بهره برداری و نهایی بوده و ضعف عمده آن‌ها به علت رفتار خطی تا لحظه شکست، در کاهش شکل پذیری مقطع می‌باشد. رفتار غیر خطی مدل سه بعدی نمونه‌های آزمایشگاهی توسط روش اجزاء محدود با استفاده از نرم افزار ANSYS مورد بررسی قرار گرفته و نمودارهای بار-خیز بدست آمده از این مدل هماهنگی قابل قبولی با نتایج آزمایشگاهی از خود نشان می‌دهد.

1. INTRODUCTION

Strengthening, upgrading and retrofitting of existing structures are among the major challenges that modern civil engineering is currently facing.

One of the most promising answers to these needs is the use of strips made of fibre reinforced polymers (FRP) bonded to the tensile face of the member. Comprehensive experimental investigations conducted in the past have shown that this

strengthening method has several advantages over the traditional ones, especially due to high strength, low weight and improved durability of the composite material.

In FRP-strengthened beams failure may occur due to beam shear, flexural compression, FRP rupture, FRP debonding or concrete cover ripping as presented by Ascione, et al [1], and Bonacci, et al [2,3]. Based on experimental results conducted by Teng, et al [4], the most common failure mode is due to debonding of FRP plate or ripping of the concrete cover. These failure modes are undesirable because the FRP plate cannot be fully utilized. In addition, such premature failures are generally associated with the reduction in deformability of the strengthened members. Premature failure modes are caused by interfacial shear and normal stress concentration at FRP cut-off points and at flexural cracks along the beam.

Extensive testing of such strengthened members has been carried out over the last two decades. A number of failure modes for RC beams bonded with FRP soffit plates have been observed in numerous experimental studies to date (e.g. Toutanji, et al [5], Saadatmanesh, et al [6], Oh, et al [7], Alagusundaramoorthy, et al [8], Chahrour, et al [9], Arduini, et al [10], Maalej, et al [11], GangaRao, et al [12], Nguyen, et al [13], Rahimi, et al [14] and Hashemi, et al [15]).

Based on existing studies, schematic representation of typical failure modes observed in tests is shown in Figure 1. These failure modes are termed: Type (1) flexural failure by crushing of compressive concrete which could happen before and/or after yielding of tensile steel reinforcement; Type (2) rupture of the FRP laminate after yielding of the steel in tension; Type (3) cover delamination at the end of FRP (shear delamination of the concrete cover); Type (4) debonding of the FRP from the concrete substrate: Type (4a) plate end interfacial debonding, Type (4b) inter-facial debonding induced by flexural crack, Type (4c) interfacial debonding induced by flexural shear crack and Type (5) shear failure.

Failure types (3) and (4a) have been studied experimentally and analytically by Maalej, et al [11], Malek, et al [16], Ascione, et al [1]. These types of failure are common in cases where the ends of the FRP sheets are not properly anchored. Failure Types (4b) and (4c) depend on the bond-

slip behaviour between FRP sheets and concrete. According to Sebastian [17] and Teng, et al [4], the corrosion of longitudinal steel bars and the change of the reinforcing bar ratio in the vicinity of large bending moments, shear forces increase the probability of these types of failures. When FRP reinforcement is being used to increase the flexural strength of a member, it is important to verify that a member will be capable of resisting the shear forces associated with the increased flexural strength. To avoid failure type 5, the potential for shear failure of the section should be considered by comparing the design shear strength of the section to the required shear strength. If additional shear strength is required, FRP laminates oriented transversely to the section can be used to resist the applied shear forces.

In spite of many recent studies on the behaviour of reinforced concrete beams strengthened using FRP composites, the effect of the reinforcing bar ratio on the behaviour and the strength of these beams has not yet been explored. The reinforcing bar ratio of beams affects the pattern and the width of cracks due to the effect of bending and shear. The influence of the FRP composites on flexural strengthening of reinforced concrete beams should depend on the width and spacing of these cracks. The ductility of beams also, depends on the reinforcing bar ratio. This paper presents the test results of six beam specimens strengthened by carbon FRP sheets. The main variable parameter in these tests are the reinforcing bar and CFRP ratio. The types of failure of these beams are also investigated.

Performing a nonlinear analysis is imperative for evaluation of structural response in terms of complete load-deflection characteristics, ductility, mode of failure and etc. particularly for earthquake engineering applications. A wide range of commercially available software like DIANA, ADINA, ATENA, ANSYS and etc. Incorporate finite elements based on nonlinear analysis capabilities incorporating both material and kinematics nonlinearities. In this paper an attempt has been made with the ANSYS software to bring into focus the versatility and powerful analytical capabilities of nonlinear FE techniques by objectively modeling the complete response of test beams.

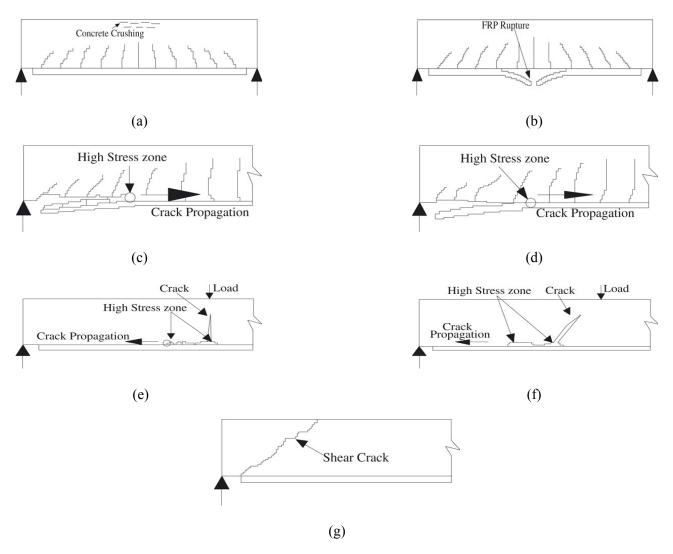The objective of this investigation is to study the effectiveness of FRP sheets on ductility and

Figure 1. Failure modes of RC beams flexurally strengthened with a FRP plate, (a) Failure type (1), (b) Failure type (2), (c) Failure type (3), (d) Failure type (4a), (e) Failure type (4b), (f) Failure type (4c) and (g) Failure type (5).

flexural strength of reinforced high strength concrete (HSC) beams. This objective is achieved by conducting the following tasks: (1) flexural testing of reinforced HSC beams strengthened with different amounts of cross-ply of FRP sheets with different amount of tensile reinforcement; (2) calculating the effect of different layouts of FRP sheets on the flexural strength; (3) evaluating the ductility index and failure modes and (4) three-dimensional nonlinear finite element models are developed to examine the test beams behavior.

2. EXPERIMENTAL PROGRAM

2.1. Material Properties   The concrete in the beams was designed for mean 28-day cube strength of about 100 MPa. For each beam three 100 mm × 100 mm × 100 mm concrete cube specimens were made at the time of casting and were kept with the beams during curing. The average 28-day concrete cube strength (f_{cu}) was 96.2 MPa. The relationship of cylinder strength (f'_c) and cube strength assumed as ($f'_c = 0.8 f_{cu}$) and

stress-strain curves for cube specimens are shown in Figure 2. Thus the average compressive strength (f'_c) was 77 MPa.

The measured yield and maximum tensile strength of the 10 and 16 mm rebar was 420.6, 634.1 and 412.5, 626.4 MPa respectively. The density and thickness of the CFRP material was 1.78 ± 0.1 gr/cm^3 and 0.045 mm respectively and 2600 mm long. The Young's modulus (E_{fu}), ultimate tensile stress (f_{fu}) and elongation (ε_{fu}) of the FRP sheets were 230 GPa, 3850 MPa and 1.7 ± 0.1 % respectively. FRP sheets externally bonded to the tension face of the concrete beams using a two-component structural epoxy named EP-TX at 1:1 ratio for the first layer and a two-part epoxy named EP-IN at 1:1 ratio for the next layer(s) of FRP. Strengthened concrete beams were cured for at least seven days at room temperature before testing.

2.2. Test Specimens   The length, width, and depth (L×b×h) of all beams were kept as 3000 × 150 × 250 mm. Each concrete beam was reinforced with two 16-mm diameter for A series and two 22-mm diameter for B series steel bars for tension and two 10-mm-diameter steel bars for compression along with 10-mm-diameter bars at a spacing of 90 mm center-to-center for shear reinforcement. The spacing of stirrups and maximum and minimum reinforcement ratios are in accordance with the provision of the American Concrete Institute (ACI).

Electrical resistance disposable strain gauges, manufactured by TML Measurements Group (Japan), were pasted on the CFRP sheets and on internal reinforcing bars at different locations. The demec and electrical gauges were also attached along the height of the beams to measure the concrete strains; these values can be used to find out the strain distribution and the moving neutral axis depth of the beams tested. All beams were loaded in four-point bending to failure with a clear span of 2.7 m, and loading points were located at 450 mm on either side of the mid-span location. The load was applied step-by-step up to failure in a load control manner of test beams. During the test, the strains on steel and concrete, and vertical deflections were measured using LVDTs. The strain gauges, LVDTs, and the load cell were connected through a data acquisition system to a computer and the data was recorded and stored in the computer (Figure 3).

For all beams, the shear-span-to-depth ratios are 4.18 and the length of the bonded plate is 2600 mm, which covers almost the full-span length between the beams supports. The reason for the full-span-length strengthening with FRP plates is to maximize the strengthening effects by delaying the FRP separation.

The main test variables considered in the present study include the FRP sheet layers and tensile bars. The FRP sheet layers varies from 0 to 4 and the bar reinforcement ratio varies from 1.2 % to 2.4 %. Of the six beams tested, two were set aside as control beams and were not strengthened (AH0, BH0), two beam were strengthened with one layer of CFRP (AH1, BH1) and two beam strengthened with four layer of CFRP (AH4, BH4) where the width of CFRP was 150 mm.

3. FINITE ELEMENT ANALYSIS APPROACH

Nonlinear FE analysis is performed using ANSYS [18], a general purpose finite element program. This section introduces the elements chosen from the software library and the analytical approach and assumptions used in the analysis.

3.1. Material Modeling   The SOLID65 [18], three-dimensional (3D) reinforced concrete solid element, is used to represent concrete in the models. This element is capable of cracking in tension and crushing in compression, although during this study, it was found that when the crushing capability of the concrete is turned on, the finite element beam models fail prematurely. Therefore, the crushing capability was turned off and cracking of the concrete controlled the failure of the finite element models.

In addition to the rebar capability of the element, the reinforcing steel can be modelled in ANSYS using a series of two node link (truss) elements, called LINK8, which has three degrees of freedom, translations of the nodal x, y, and z directions, which is also capable of plastic deformation. Unlike concrete, steel is very uniform and as such generally the specification of a single
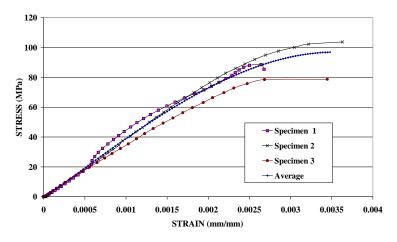
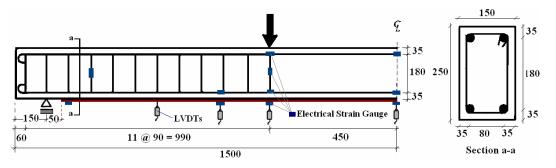**Figure 2**. Stress-strain diagram for high strength concrete.

Figure 3. Beam details and measurement schemes for half of
the test specimen (unit: millimeter).

stress-strain relation is adequate to define it numerically. For this, the nonlinear stress-strain relation was approximated by a series of straight line segments in such a way that the critical part of the curve, such as onset of steel yielding and strain hardening, were simulated by piecewise linear models.

The SOLID46, 3D layered structural solid element, is used to represent the FRP materials. The element has eight nodes with three translational DOFs at each node. Assuming perfect interlaminate bond, no slippage is allowed between the element layers. The FRP laminates are considered brittle materials, and the stress-strain relationship is roughly linear up to failure. Consequently, in this study it is assumed that the stress-strain relationships for the FRP laminates are linearly

elastic. Finite element analysis approach reported by Hashemi, et al [15].

4. COMPARISON BETWEEN EXPERIMENTAL DATA AND NUMERICAL RESULTS

4.1. Load-Displacement Curves In this section; the numerical results for all specimens are presented and compared with experimental values. Figures 4 and 5 contain a comparison between the load-displacement curves predicted by ANSYS and the test results for all specimens. As is seen, the agreement is reasonable. The results of ANSYS match the plain specimen better than the
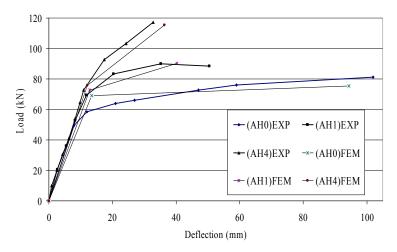
Figure 4. Comparison between load-displacement curves predicted by ANSYS and the test result for the A group specimens.
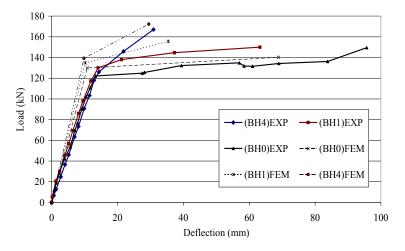

Figure 5. Comparison between load-displacement curves predicted by ANSYS and the test result for the B group specimens.

strengthened specimens. This may be as a result of bond slip between FRP and concrete that is ignored in the current analysis.

In general, the strengthened beams were stiffer and less ductile than the control specimens with a higher ultimate load. As a result compared to a beam reinforced heavily with steel only, beams reinforced with both steel and CFRP have adequate deformation capacity, in spite of their brittle mode of failure. The predicted results are compared with the experimental load and deflection, as graphically

shown in Figures 6 and 7. It can be seen that the finite element model predicts the load and deflection very well.

4.2. Failure Pattern The cracking patterns and failure for various test beams are shown in Figure 8. The control beams without strengthening plates was designed to fail in flexure. For the control beams (AH0, BH0), failure was by crushing of the concrete in the compression zone after the tensioned steel yield.
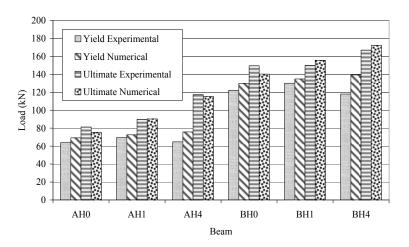
Figure 6. Comparison between experimental and numerical yielding and ultimate load.
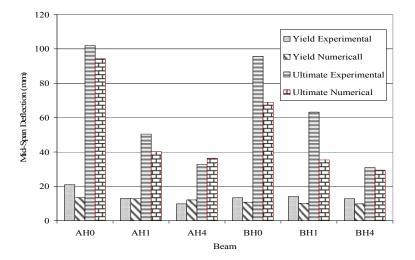

Figure 7. Comparison between experimental and numerical yielding and ultimate deflection.

All of the strengthened test beams exhibited the rupture of FRP sheets and failed in the same manner. We attended the failure of a concrete cover along the tensile reinforcement. The concrete was not initially pre-cracked and the development of the cracks during the reinforcement test is highly influenced by the number of CFRP layer. The occurrence of the first crack was delayed and more diffused. Shear cracks occurred in the shear span length of the beams for an applied load "Between" 70 % to 80 % of the ultimate load. Finally the sudden propagation of horizontal cracks

in the concrete-steel bond region occurs. This type of cracks runs along the weakest surface, which is the concrete-steel interface. It leads to the failure of the beam as soon as the cracks opened and separates the concrete cover from the rest of the beam. It is interesting to note that the weakest point of the assemblage concrete-bond-composite material is not the concrete-composite interface but the concrete-internal steel interface.

From the experimental observation, it can be seen that the bond between FRP and concrete is strong enough to ensure the rupture of the
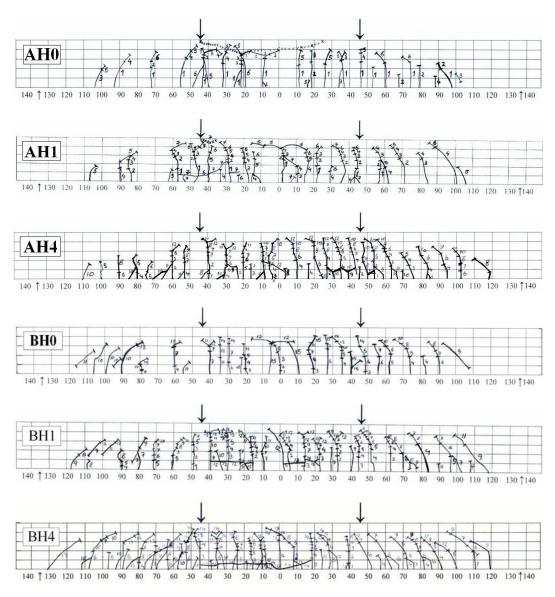
Figure 8. Failure configuration of control and FRP beams at ultimate state.

composites, thus when four or less than four layers of carbon fibre are applied, the bonding is not the controlling factor for failure, thus the force in FRP will reach its ultimate tensile capacity when the beam fails, the concrete node with the FRP node in finite element model is a true assumption.

The tensioned steel in control beams AH0 and BH0 reached its yield strength before the compressive strain in concrete reached 0.003 and the beams failed by concrete crushing. Even though the control beams failed by crushing

concrete, the failure was initiated by the yielding of tensioned steel, the mode of failure was mentioned to be under reinforced tension failure thus the behavior of the two control beams was a ductile flexural response. For control beams after the first visible cracks were observed, the cracking became extensive and crack widths increased steadily. The shape of the load deflection curves indicates a loss of stiffness at a load of approximately 64 kN for AH0 and 122 KN for BH0. This was due to yielding of the tensile

reinforcement and occurred at a mid-span deflection of 21 mm for AH0 and 13.3 mm for BH0. After this point, large flexural cracks opened during the test and eventual ultimate collapse occured by concrete crushing within the compression zone, a photograph of which is presented in Figure 9. The ultimate loads recorded were 81.25 and 149.5 kN for AH0 and BH0, respectively.

In this study, for AH1, AH4, BH1 and BH4 the bond problem is not the controlling factor for failure, thus the force in CFRP will reach its ultimate tensile capacity when the beam fails and the failure mode of the strengthened beams are CFRP rupture in the constant moment region. Figyres 10a,b shows such a typical failure mode.

4.3. Discussions on Flexural Behavior   As a result, when FRPs are used for flexural strengthening of concrete beams reinforced with conventional steel, the steel reinforcement may yield before the FRP contributes any additional capacity to the beam. Therefore, it can be difficult to obtain a significant increase in yield load or stiffness for a beam.
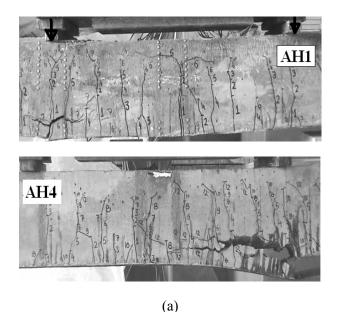
When an increase in beam yield load or stiffness is required, larger cross sections of FRPs must be used (before the steel yields), which generally increases the cost of strengthening. Although using some special, low-strain fibres, such as ultra-high-modulus carbon fibres, may appear to be a solution; they can result in brittle failures due to fibre failure. Taking advantage of high strength FRPs during flexural strengthening of RC beams is limited by the bond capacity between them and the concrete surface.
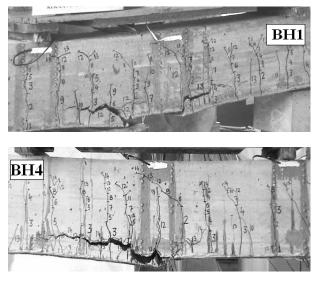
Table 1 shows a summary of the flexural behavior of all test beams in terms of flexural loading capacity and deflection. The results clearly demonstrated the accepted beneficial effects of CFRP layers with regard to stiffening and strengthening of the beams. Table 2 shows the increase of peak load according to the various strengthening layers of CFRP. The rates of increase in peak loads varied from 1 to 44 % for experimental data and 11 to 53 % for numerical results depending on the strengthening method.

As the amount of steel reinforcement increases, the additional strength provided by the carbon FRP external reinforcement decreases. The same amount

Figure 9. Flexural failure of control beam AH0.

(a)

(b)

Figure 10. (a) Rupture of FRP in beams AH1, AH4, (b) Rupture of FRP in beams BH1, BH4.

TABLE 1. Numerical and Experimental Mid-Span Deflection and Load in Yield and Ultimate Stage of RC Beams Strengthened with CFRP Sheets.

Source	Test Beam	Yield Stage				Ultimate Stage			
		Load P_y(kN)	Increase Over Control (%)	δ_y(mm)	Decrease Over Control (%)	Load P_u(kN)	Increase Over Control (%)	δ_u(mm)	Decrease Over Control (%)
Exp	AH0	63.93	---	21	---	81.25	---	102	---
	AH1	69.5	8.7	13	38	89.9	11	50.42	51
	AH4	64.7	1.2	9.83	53.2	117.3	44.4	32.85	67.8
Num	AH0	69.2	---	13.5	---	75.4	---	94.3	---
	AH1	72.6	4.9	12.8	5.2	90.2	19.6	40.25	57.4
	AH4	75.7	9.4	12.1	10.4	115.4	53.05	36.4	61.4
Exp	BH0	122.2	---	13.325	---	149.52	---	95.7	---
	BH1	130	6.4	14.11	-5.9	150	0.5	63.24	33.9
	BH4	118	-3.4	12.86	3.6	167	11.7	30.92	67.7
Num	BH0	129.9	---	10.8	---	140.2	---	68.9	---
	BH1	134.8	3.7	10.2	5.6	155.6	10.9	35.4	48.7
	BH4	139.2	7.1	9.8	9.1	172.3	22.9	29.5	57.2

TABLE 2. Experimental and Numerical Ductility Ratio of the Test Beams.

Series	Test Beam	Elastic Energy (E_y) (ton.mm)	Failure Energy (E_U) (ton.mm)	Energy Ductility Ratio $\left(\dfrac{E_U}{E_y}\right)$	Deflection Ductility Ratio $\left(\mu_\delta = \dfrac{\delta_u}{\delta_y}\right)$		Decrease Over Control Beam (%)	Curvature Ductility Ratio $\left(\mu_\phi = \dfrac{\phi_u}{\phi_y}\right)$
					EXP	FEM		
A	AH0	104.9	718.03	6.85	4.86	6.98	----	6.37
	AH1	53.5	354.1	6.62	3.87	3.14	20.4	----
	AH4	34.3	259.3	7.56	3.34	3.01	31.3	3.91
B	BH0	90.2	1181.7	13.1	7.19	6.38	----	6.2
	BH1	99.6	755.3	7.58	4.48	3.47	37.7	----
	BH4	74.9	344.23	4.59	2.4	3.01	66.6	2.37

of CFRP reinforcement more than 44 % the flexural strength of a lightly reinforced beam (ρ = 1.2 %), but the strength of a moderately reinforced beam only increased by 11.7 % (ρ = 2.4 %).

4.4. Ductility Ductility is an important factor for any structural element or structure itself especially in the seismic regions. A ductile material is one

that can undergo large strains while resisting loads. When applied to RC members, the term ductility implies the ability to sustain significant inelastic deformation prior to collapse. In the case of beams strengthened with FRP laminates, there is usually no clear yield point. However, it was shown that deflection and energy based on tension steel yielding can be used as a criterion of ductility to

evaluate comparative structural performance of FRP bonded RC beams [12]. Figure 11 schematically shows the response of a strengthened RC beam. Point A corresponds to first concrete cracking, point B to first steel yielding, and point C to failure.

The energy ductility index (D_E) is defined as the ratio between the energy of the system at failure (E_U) and the energy of the system at first steel yield (E_y).

The other definitions of ductility index in this study is obtained based on deflection (μ_d) and curvature (μ_ϕ) computation, and is defined as the mid-span deflection or curvature, at peak load, divided by the mid-span deflection or curvature at the point where the steel starts yielding.

Table 1 shows the experimental and numerical yielding results of the beams and the ultimate stage. Table 2 shows the experimental energy, deflection and curvature ductility ratio and the decrease percentage of ductility with respect to the control beam for each of the specimens. Table 2 also shows the deflection ductility ratio based on finite element model results.

Reinforced concrete structures usually behave in a ductile manner if an appropriate amount of steel reinforcement is added. Ductility is achieved by inelastic deformation of the steel before failure. During this period, the concrete beam consumes much of the energy causing the elastic energy released at failure to be reduced. However, this is not the same circumstance for FRP reinforced beams, since this material can not usu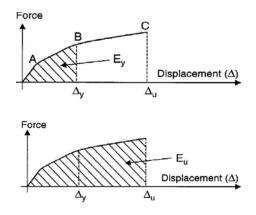ally attain inelastic deformation. This causes a tremendous amount of elastic strain energy to build up and be released at failure which exceeds that of steel reinforcement.

As seen in the Table 2, by comparison between energy and displacement ductility ratio, it was found that for all the beams reported, the energy ductility values is about two times higher than the displacement ductility values. Thus, the energy ductility index, proposed in this study is as follows and Table 3 lists the value of energy ductility index proposed in this study.

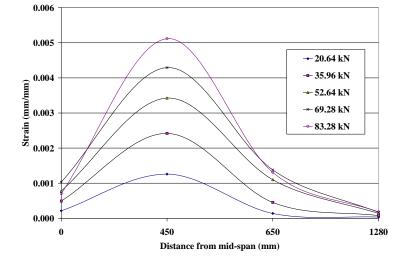$$\mu_E = \frac{1}{2}\left(\frac{E_U}{E_y} + 1 \right)$$

Considering HSC members, displacement ductility, μ_d, in the range of 3 to 5 is considered imperative for adequate ductility, especially in the areas of seismic design and the redistribution of moments [20]. Therefore, assuming that a μ_d value of 3 represents an acceptable lower bound to ensuring the ductile behavior of HSC flexural members, it appears that, for the BH4 beam would not meet that requirement. As seen in Table 3, brittle failure mode cause that flexural strengthening of an over reinforced RC beam may not be a viable solution and when dealing with an under reinforced RC beam, its strengthening should not make it over reinforced.

4.5. CFRP Strain   The variations in longitudinal strain in the CFRP sheet from the mid-span of the beam to the end of the sheet, as a function of the changes in externally applied load, for A series test beam, are plotted in Figures 12a,b. Generally the strain in the constant bending moment region was sensibly uniform for a given load, although the strains under the load points, due to the localized loading points, were slightly higher than those recorded at the mid-span. Within the shear span, the strain drops almost linearly from a maximum under the load point to a zero at the end of the sheet. This pattern of strain distribution in the bonded plate was typical of each test beam. Similar results are reported by Fanning, et al [21].
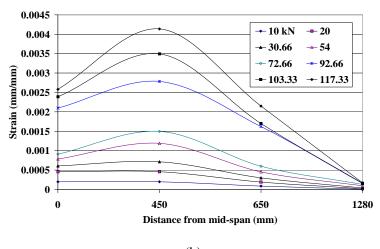
4.6. Concrete Load-Strain Response at Mid-Span   The relationship between concrete strains (measured on the compression face at mid-span)

Figure 11. Definition of energy ductility [19].

TABLE 3. Proposed Energy Ductility Ratios of the Test Beams.

Series	Test Beam	Energy Ductility Ratio $\mu_E = \dfrac{1}{2}\left(\dfrac{E_U}{E_y}+1\right)$	Deflection Ductility Ratio $\left(\mu_\delta = \dfrac{\delta_u}{\delta_y}\right)$	$\dfrac{\mu_E}{\mu_\delta}$
A	AH0	3.92	4.86	0.81
	AH1	3.81	3.87	0.98
	AH4	4.28	3.34	1.28
B	BH0	7.05	7.19	0.98
	BH1	4.29	4.48	0.96
	BH4	2.8	2.4	1.17

(a)

(b)

Figure 12. (a) CFRP strain distribution for beam AH1 and (b) CFRP strain distribution for beam AH4.

and applied load for both A and B series are measured from experimental and finite element model plotted in Figures 13 and 14. There is a similar increase in strain for all the beams at low moments. However, cracking of the concrete in the tension zone results in larger increments of strain in the control specimens (i.e., for control beam AH0, the extreme layer of concrete compressive strain at failure, ε_{cuf} = 0.0036). For these beams, concrete strain varies almost linearly with moment, after initial cracking, until yielding of the steel tension.

Following yield, steel strain increases rapidly with each increment of load, and finally the
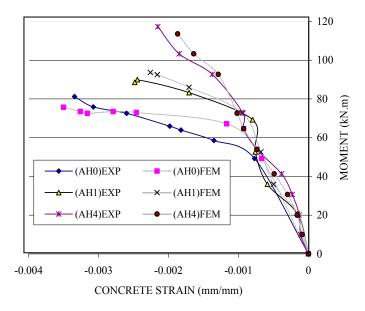

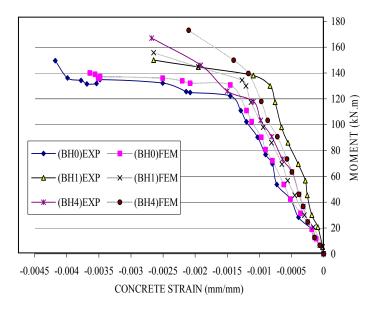**Figure 13**. Experimental and analytical load vs. concrete strain at mid-span for A group.

Figure 14. Experimental and analytical load vs. concrete strain at mid-span for B group.

concrete crushes as the beam collapses (see Figure 9). On the other hand, the extreme compressive strain of concrete fiber in the strengthened beams with the increased number of layers of the CFRP sheet remains more or less linear up to failure and is not significantly affected by concrete cracking or yielding of the steel tension. These results demonstrate that the effect of the strengthening plate is to reduce strain in the compression fibres of the concrete. The presence of the plate draws the neutral axis lower in the section and, hence, places a greater volume of concrete in compression, resulting in lower strain (see Figures 13 and 14) and enabling a more efficient use of the existing material. Thus, externally bonded CFRP plates may also be beneficially used to reduce concrete compressive stresses, in addition to acting as additional tensile reinforcement.

The relationship between concrete, CFRP and tensile bar steel strains (measured at mid-span) and applied moment for AH4 and BH4 beams measured from experimental study are plotted in Figure 15.

Figure 15 indicates that each curve consists of almost three straight lines with different slopes. The first turning point, A, indicates the cracking of concrete in tension zone. The second turning point, B, refers to the yielding tension steel. The yielding

and maximum load (ultimate load) can be found for each beam from its load-strain curve.

For beams AH4 and BH4, the tensile steel and CFRP strains are essentially the same at loads below cracking of the concrete. After cracking, the strains in steel exceeded those of the CFRP laminate. As the load approached the yielding load for the strengthened beam, the strains in steel increased more rapidly than those in the CFRP. This is because the CFRP had begun to debond from the concrete surfaces' nearby cracks. It was noted that the tensile steels strains were always higher than the CFRP strains.

5. CONCLUSIONS

The major conclusions derived from this experimental study are given as follows:

- The finite element model results show good agreement with observations and data from the experimental full-scale beam tests. This numerical study can be used to predict the behavior of reinforced concrete beam strengthened with FRP more precisely by assigning appropriate material properties
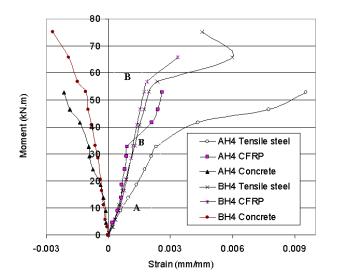

Figure 15. Moment-strain curve of CFRP, tensile steel and extreme top concrete fibre for beam AH4 and BH4 at mid-span section.

to develop design rules for strengthening RC member using FRP.

- The results of tests performed in this study indicate that significant increase in the flexural strength can be achieved by bonding CFRP sheets to the tension face of high strength reinforced concrete beams. The gain in the ultimate flexural strength was more significant in beams with lower steel reinforcement ratios.

- It was found that for all strengthened test beams, that the tensile steels strains were always higher than the CFRP strains.

- The extreme compressive strain of concrete fibre in the strengthened beams with increased number of CFRP layers remains more or less linear, up to failure of the beam and is not significantly affected by concrete cracking or yielding of the tension steel. These results demonstrate that the effect of strengthening plate is to reduce strain in the compression fibres of the concrete.

- Comparing a beam reinforced heavily only with steel with a beam reinforced with both steel and CFRP would have adequate deformation capacity, in spite of their brittle mode of failure.

- As the amount of tensile steel reinforcement increases, the additional strength provided by the carbon FRP, external reinforcement decreases.

- The same amount of CFRP reinforcement more than 44.4 % of the flexural strength of a lightly reinforced beam (20 % of balanced ratio), only increased by 11.7 % the strength of a moderately reinforced beam (40 % of balanced ratio).

- It was found that for all the beams reported, the energy ductility values is about two times higher than the displacement ductility values.

- Generally the CFRP strain in the constant bending moment region was sensibly uniform for a given load, although the strains under the load points, due to the localized loading points, were slightly higher than those recorded at the mid-span. Within the shear span, the strain drops almost linearly from a maximum under the load point to a zero at the end of the sheet.

6. REFERENCES

1. Ascione, L. and Feo, L., "Modeling of Composite Concrete Interface of RC Beams Strengthened with Composite Laminates", *Composites Part B. Engineering*, Vol. 31, (2000), 535-540.
2. Bonacci, J.F. and Maalej, M., "Externally Bonded Fiber-Reinforced Polymer for Rehabilitation of Corrosion Damaged Concrete Beams", *ACI Structural Journal*, Vol. 97, No. 5, (2000), 703-711.
3. Bonacci, J.F. and Maalej, M., "Behavioral Trends of RC Beams Strengthened with Externally Bonded FRP", *Journal of Composite for Construction*, Vol. 5, No. 2, (2001), 102-113.
4. Teng, J.G., Smith, S.T., Yao, J. and Chen, J.F., "Intermediate Crack-Induced Debonding in RC Beams and Slabs", *Construction and Building Materials*, Vol. 17, (2003), 447-62.
5. Toutanji, H., Zhao, L. and Anselm, E., "Verifications of Design Equations of Beams Externally Strengthened with FRP Composites", *Journal of Composites for Construction*, Vol. 10, No. 3, (2006), 254-264.
6. Saadatmanesh, H. and Ehsani, M.R., "RC Beams Strengthened with GFRP Plates. I: Experimental Study", *Journal of Structural Engineering*, Vol. 117, No. 11, (1991), 3417-3433.
7. Oh, B.H., Cho J. Y. and Park, D.G., "Static and Fatigue Behavior of Reinforced Concrete Beams Strengthened with Steel Plates for Fexure", *Journal of Structural Engineering*, Vol. 129, No. 4, (2003), 527-535.
8. Alagusundaramoorthy, P., Harik, I.E. and Choo, C.C., "Flexural Behavior of RC Beams Strengthened with Carbon Fiber Reinforced Polymer Sheets or Fabric", *Journal of Composites for Construction*, Vol. 7, No. 4, (2003), 292-301.
9. Chahrour, A. and Soudki, K., "Flexural Response of Reinforced Concrete Beams Strengthened with End-Anchored Partially Bonded Carbon Fiber-Reinforced Polymer Strips", *Journal of Composites for Construction*, Vol. 9, No. 2, (2005), 170-177.
10. Arduini, M. and Nanni, A., "Behavior of Pre-Cracked RC Beams Strengthened with Carbon FRP Sheets", *Journal of Composites for Construction*, Vol. 1, No. 2, (1997), 63-70.
11. Maalej, M. and Bian, Y., "Interfacial Shear Stress Concentration in FRP Strengthened Beams", *Composite Structures*, Vol. 54, (2001), 417-426.
12. GangaRao, H.V.S. and Vijay, P.V., "Bending Behavior of Concrete Beams Wrapped with Carbon Fabric", *Journal of Structural Engineering*, Vol. 124, No. 1, (1998), 3-10.
13. Nguyen, D.M., Chan, T.K. and Cheong, H.K., "Brittle Failure and Bond Development Length of CFRP-Concrete Beams", *Journal of Composites for Construction*, Vol. 5, No. 1, (2001), 12-17.
14. Rahimi, H. and Hutchinson, A., "Concrete Beams Strengthened with Externally Bonded FRP Plates", *Journal of Composites for Construction*, Vol. 5, No. 1, (2001), 44-56.
15. Hashemi, S.H., Rahgozar, R. and Maghsoudi, A.A., "Finite Element and Experimental Serviceability Analysis

of HSC Beams Strengthened with FRP Sheets", *American Journal of Applied Sciences*, Vol. 4, No. 9, (2007), 725-735.

16. Malek, A.M., Saadatmanesh, H. and Ehsani, M.R., "Prediction of Failure Load of RC Beams Strengthened with FRP Plate Due to Stress Concentration at the Plate End", *ACI Structural Journal*, Vol. 95, No. 2, (1998), 142-152.

17. Sebastian, W.M., "Significance of Mid-Span Debonding Failure in FRP-Plated Concrete Beams", *Journal of Structural Engineering*, Vol. 127, No. 7, (2001), 792-798.

18. ANSYS, I. "ANSYS Manual Set", ANSYS, Inc., Canonsburg, PA 15317, U.S.A., (2003).

19. Thomsen, H.H., Spacone, E., Limkatanyu, S. and Camata, G., "Failure Mode Analysis of Reinforced Concrete Beams Strengthened in Flexure with Externally Bonded Fibre-Reinforced Polymers", *Journal of Composites for Construction*, Vol. 8, No. 2, (2004), 123-131.

20. Maghsoudi, A.A. and Akbarzadeh, H., "Flexural Ductility of HSC Members", *Structural Engineering and Mechanics an International Journal*, Vol. 24, No. 2, (2006), 195-213.

21. Fanning, P.J. and Kelly, O., "Ultimate Response of RC Beams Strengthened with CFRP Plates", *Journal of Composites for Construction*, Vol. 5, No. 2, (2001), 122-127.